# PROCEDURE FOR SMOOTHING MPSI STRESS STRAIN CURVES

BY

JAMES F. DORRIS

AND

JACQUE S. AUSTIN

APRIL, 1983

DRAFT REPORT

## TABLE OF CONTENTS



## LIST OF ILLUSTRATIONS

## LIST OF TABLES

# PROCEDURE FOR SMOOTHING MPSI STRESS STRAIN CURVES

## INTRODUCTION

In Phase I of the Mechanical Properties of Sea Ice (MPSI) program, approximately 240 uniaxial constant strain rate compression tests were conducted. These tests were recorded on a FM magnetic tape recorder. It was necessary to digitize the analog magnetic tapes in order to employ a computer analysis of the data. After digitization, the data were processed further by fitting cubic splines to the digital data from each test. This step serves three purposes:

1. Cubic splines provide a more efficient means of storing the data,
2. any noise in the data is filtered out, and
3. application of constitutive models to ice requires an analytical description of the stress-strain curve.

The following account describes the procedures employed in obtaining the smooth stress strain curves from the digitized data. The procedures describing the digitization process will be documented later.

## CUBIC SPLINES

The cubic splines for each test are found by employing the IMSL subroutine ICSVKU. This subroutine requires that the range of the independent variable, t, be divided into (k-1) intervals by selecting k knots, $t_i$, i=1,2,...,k. The subroutine then calculates a cubic spline $S_i$ for each interval. Taken together, the splines form a (k-1) branched composite function, F(t), which is continuous and has continuous first and second derivatives at each intermediate knot. The cubic splines are chosen so that the composite function minimizes the least squares error of the approximation to the digitized data.

Each spline, $S_i$, is referred to a local coordinate system, $(\xi_i, S_i(\xi_i))$ whose origin is located at the point $(t_i,0)$. To evaluate the composite

function at the point $t=\hat{t}$, one must first find the knot interval, $I_i$: $t_i \leq \hat{t} \leq t_{i+1}$, in which the point lies. Once this interval is found the function is evaluated by the equation,

$$S_i(\hat{\xi}_i) = \left[\left(C_{i3}\,\hat{\xi}_i + C_{i2}\right)\hat{\xi} + C_{i1}\right]\hat{\xi}_i + y_i, \qquad (1)$$

where $\hat{\xi}_i = \hat{t} - t_i$, $0 \leq \hat{\xi}_i \leq t_{i+1} - t_i$.

Here $C_{i3}$, $C_{i2}$, and $C_{i1}$ are the cubic, quadratic, and linear coefficients, respectively of the local independent variable, $\xi_i$. The quantity, $y_i$, denotes the initial value of the spline in the local coordinate system. These quantities are returned by the subroutine and represent the best fit of the data on the interval, $t_i \leq t \leq t_{i+1}$. The (k-1)x3 matrix $C_{ij}$, the (k-1) dimensional vector $y_i$, and the k dimensional vector $t_i$ will completely specify the composite function, F(t). These quantities will be tabulated in data files for each test. A schematic diagram of the composite function and cubic splines is found in Figure 1.

The successful use of splines to approximate a data set is dependent on the choice of knots. The subroutine ICSVKU is a variable knot routine which optimizes the knot locations after an initial guess is made for the knots. The IMSL library package also contains several subroutines which evaluate the splines, take first and second derivatives, and integrate. However, it is not necessary to have access to the IMSL library package to perform these calculations, since it is an easy task to program Equation (1) if given the quantities $C_{ij}$, $y_i$, and $t_i$.

## TEST MEASUREMENTS

In Phase I, the uniaxial compression tests were conducted at strain rates, $\dot{\varepsilon}$, of $10^{-5}$/sec and $10^{-3}$/sec, and temperatures, $\Theta$, of $-5^{\circ}$C and $-20^{\circ}$C. Each test sample was loaded at a constant strain rate until either the sample failed or the strain reached 5%. The shape of the stress strain curve is highly dependent on strain rate and much less dependent on temperature. Consequently, for the purpose of curve fitting, we will only consider the two strain rates to be the test

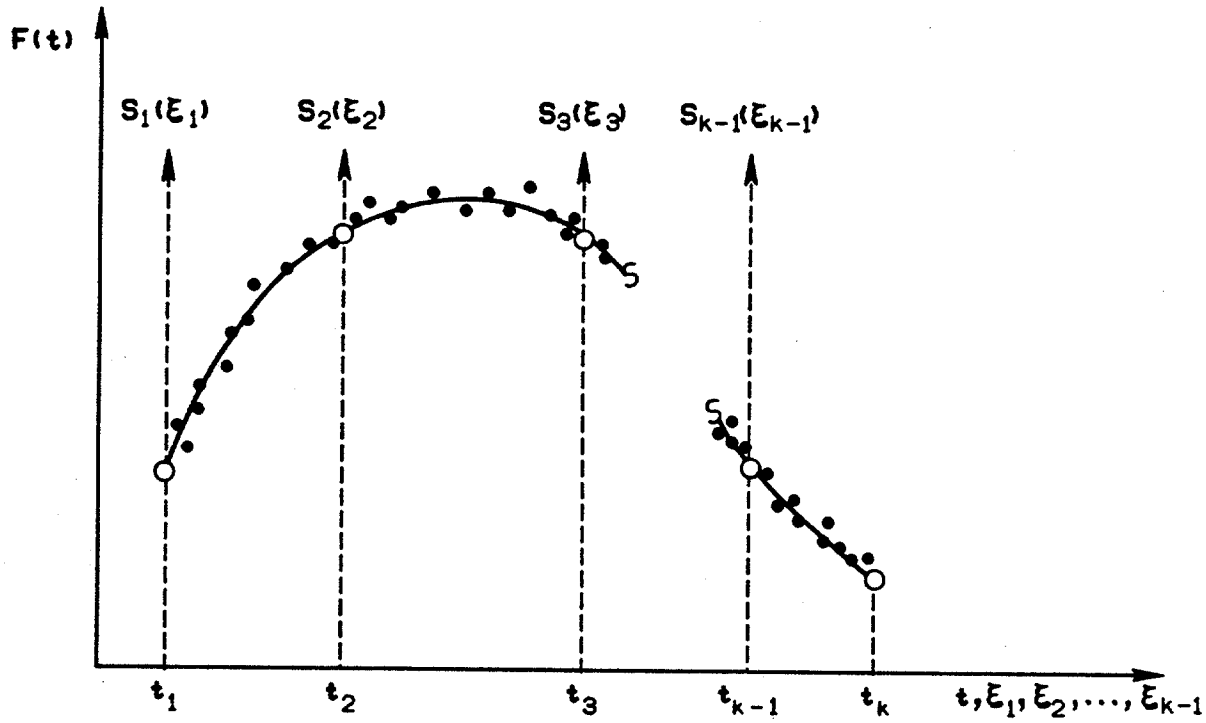


$$F(t) = \begin{cases} S_1(\xi_1) & , \ 0 \le \xi_1 \le t_2 - t_1 \\ S_2(\xi_2) & , \ 0 \le \xi_2 \le t_3 - t_2 \\ S_3(\xi_3) & , \ 0 \le \xi_3 \le t_4 - t_3 \\ \vdots & \qquad \vdots \\ S_{k-1}(\xi_{k-1}) & , \ 0 \le \xi_{k-1} \le t_k - t_{k-1} \end{cases} \quad t_1 \le t \le t_k$$

WHERE,

$$S_i(\xi_i) = \left\{ \left[ C(i,3)\xi_i + C(i,2) \right] \xi_i + C(i,1) \right\} \xi_i + y_i$$

84-228-1
ADS/SC
DORRIS

Fig. 1 - Typical spline fit to experimental data.

conditions. All observations or conclusions regarding tests at a given strain rate will apply to both temperatures. In the following, two tests are chosen to be typical examples of the results from each of the two strain rates. Test number R5A-165/191 will represent the $10^{-5}$/sec tests and test number R4B-299/325 will represent the $10^{-3}$/sec tests.

In each test, a load cell recorded the axial force as a function of time. The axial displacement was also recorded as a function of time with an extensometer and two DCDT's. The extensometer recorded displacements over the full sample length (10 in.) and was used as the feedback control on the closed loop testing machine. The two DCDT's were mounted on the ice sample 180° apart with a 5½" gauge length. The calibrated output from the load cell is converted to stress by dividing by the original cross sectional area of the sample and the calibrated output from the axial displacement transducers is converted to strain by dividing by the appropriate gauge length.

In Figures 2 and 3, the strain recorded from each axial displacement transducer is recorded as a function of time for each strain rate. At the beginning of each test, there is close agreement between all three transducers, but there is a point at which the output of the two DCDT's begins to diverge from the extensometer. This point is usually just prior to the peak force. Ideally for a constant strain rate test, the DCDT's should produce linear measurements similar to the extensometer throughout the test. However, at times corresponding to the peak force, the ice begins to undergo nonhomogeneous deformations characterized by highly localized bulging and fracturing. Since the DCDT's are attached directly to the ice, their nonlinear measurements are a direct result of the nonhomogeneous deformations. For this reason the measurements from the DCDT's should not be considered dependable beyond the initial portion of the test. The extensometer, on the other hand, measures the relative displacement of the endcaps and its measurements should be interpreted as the average displacement over the sample length. Since we are interested in constant strain rate up to 5% strain, only the extensometer will be used to measure axial displacement.

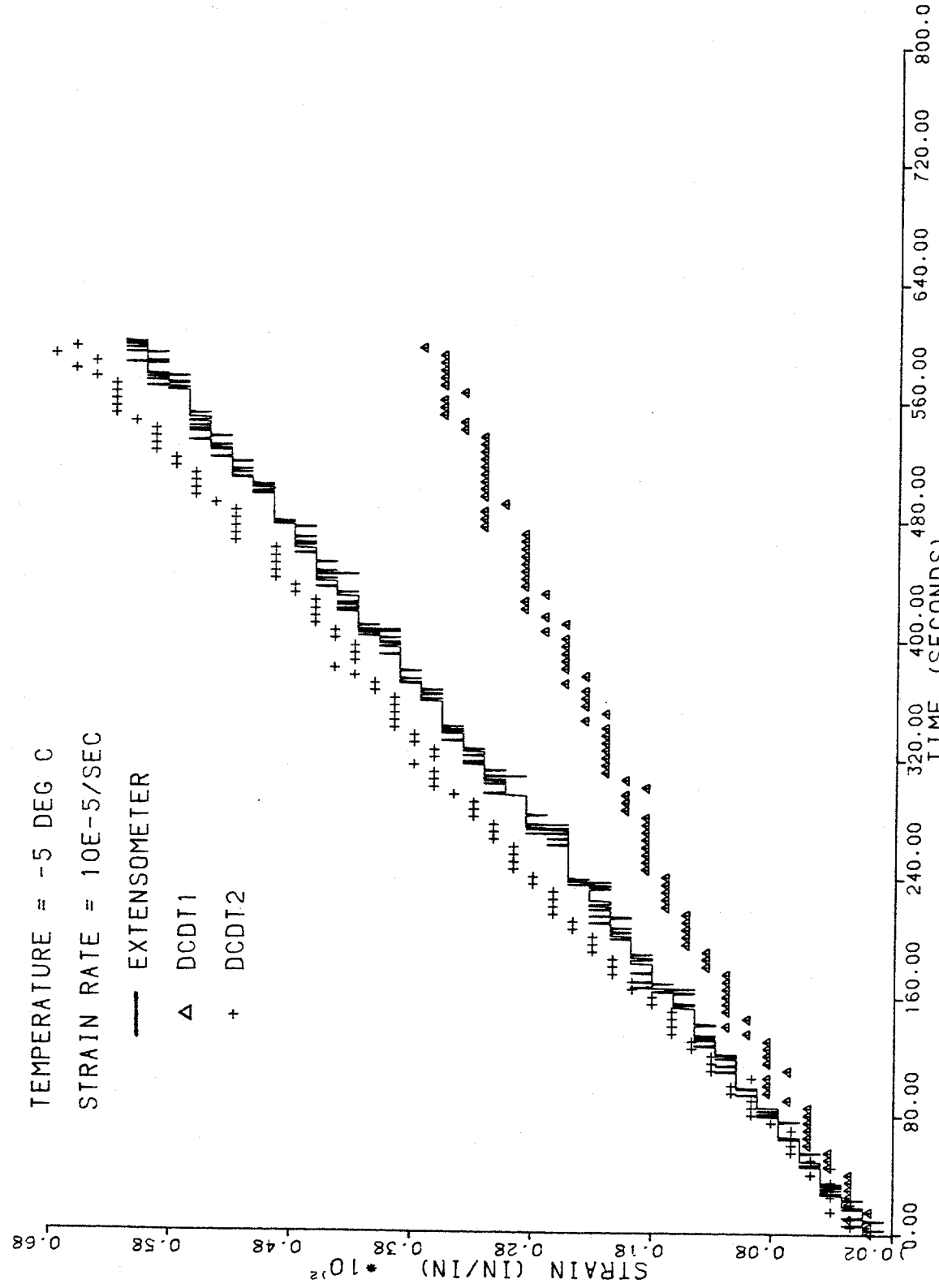


Fig. 2 - Enlarged view near the origin of the strain measured by the extensometer and the two DCDT's for a $10^{-5}$/sec test.

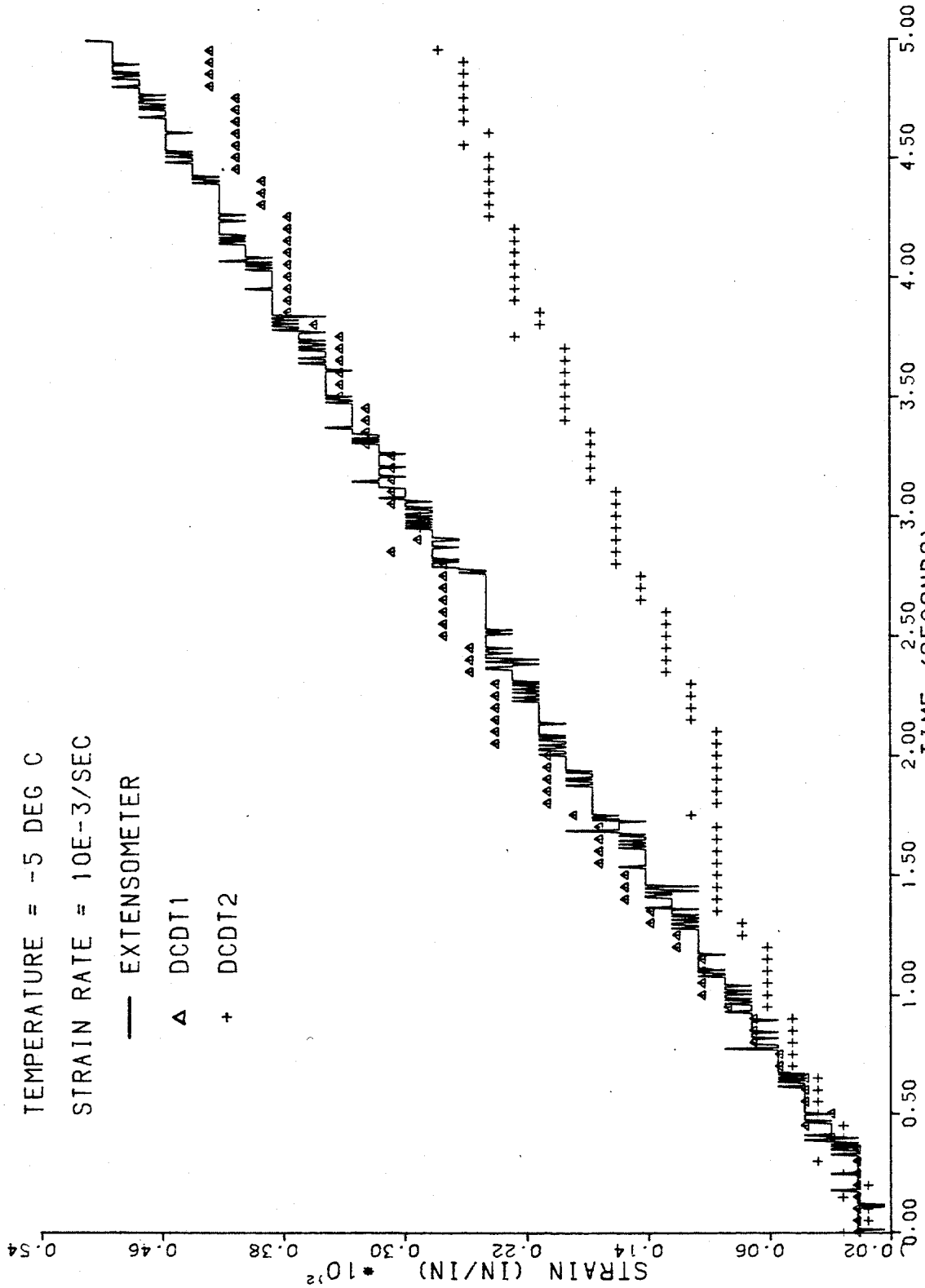


Fig. 3 - Enlarged view near the origin of the strain measured by the extensometer and the two DCDT's for a $10^{-3}$/sec test.

The complete time histories for the load and strain measured from the extensometer are shown in Figures 4 and 5 for each strain rate. The force histories for each strain rate are plotted on the same coordinate axes in Figure 6 to illustrate the change in shape with strain rate. As will be seen later, the differences in shape will require slightly different fitting techniques for each strain rate.

## FITTING PROCEDURES FOR FORCE-TIME CURVES

When conducting an experiment, the experimentalist attempts to create an idealized situation to obtain measurements for use in a theoretical model or hypothesis. But, because of experimental limitations, it is usually impossible to create these ideal situations, causing some discrepancies between experiment and theory which should be accounted for in the data analysis.

To illustrate some of the discrepancies arising the uniaxial compression tests, consider Figures 7-10 which show enlarged views of the force and strain measurements near the beginning of each test. In Figures 7 and 9, the force increases from zero at time, t=0, as expected whereas in Figures 8 and 10 the axial displacement does not increase from zero until approximately t=8 sec for the $10^{-5}$/sec tests and t=0.3 sec for the $10^{-3}$/sec tests. This apparent discrepancy in the starting time is due to the finite amount of time required for the machine to overcome the initial condition of being at rest and then reach a steady state condition of constant strain rate. Figures 7 and 9 also show the initial curvature (i.e. the second derivative) of the force-time curves to be positive. This initial positive curvature is partly due to the initially nonconstant strain rate and is partly due to the elastic closure of voids and microcracks which acts to stiffen the material response. Because of the positive curvature, the maximum slope would occur sometime after the beginning of the test. This contradicts constitutive theories (e.g. elasto-plasticity, viscoelasticity, etc.) commonly used to describe materials having nonlinear stress-strain curves. These theories assume the maximum slope occurs at the beginning of the test and represents the initial elastic response of the material.

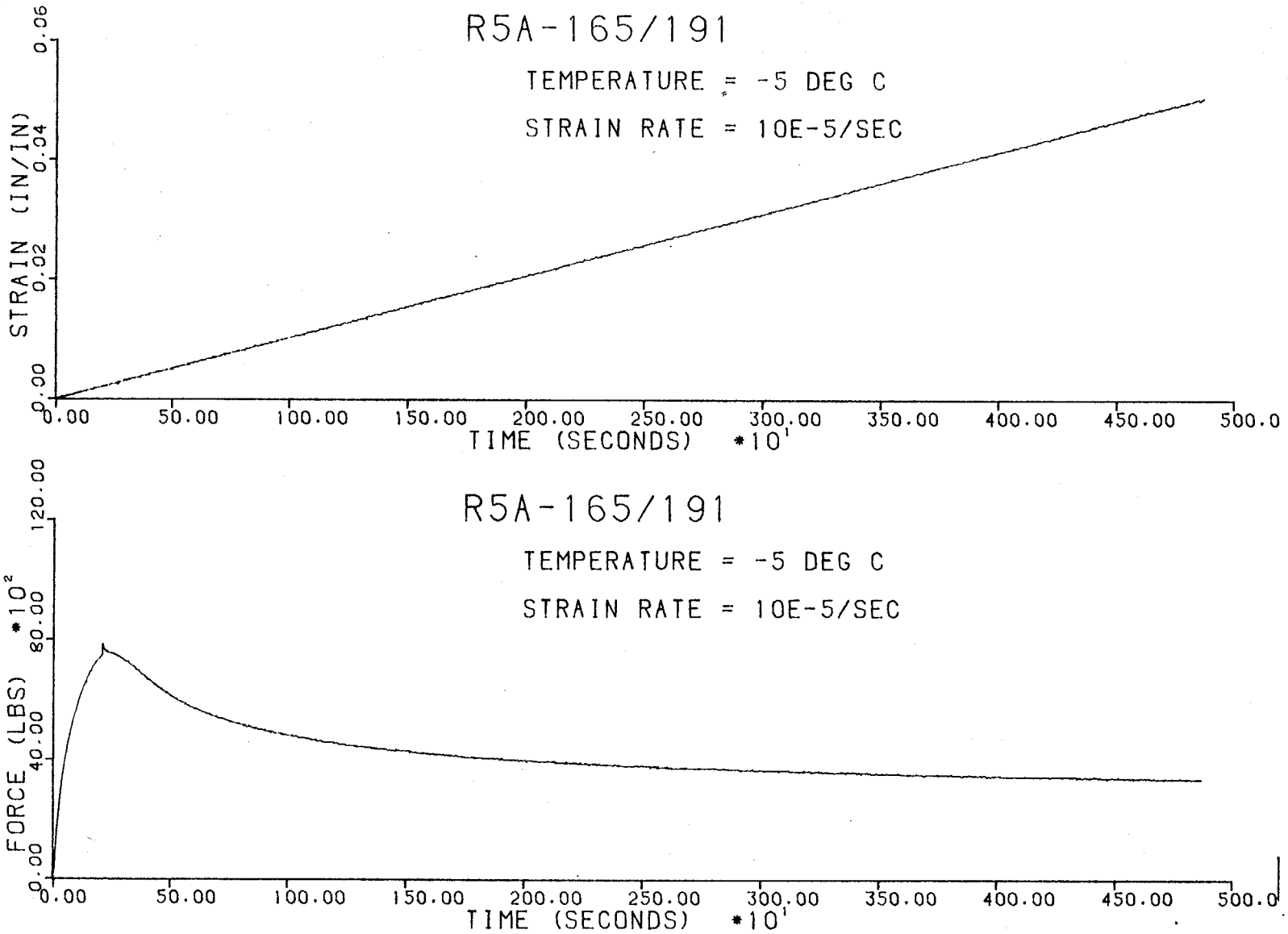


Fig. 4 - Measured strain and force histories for a $10^{-5}$/sec test.

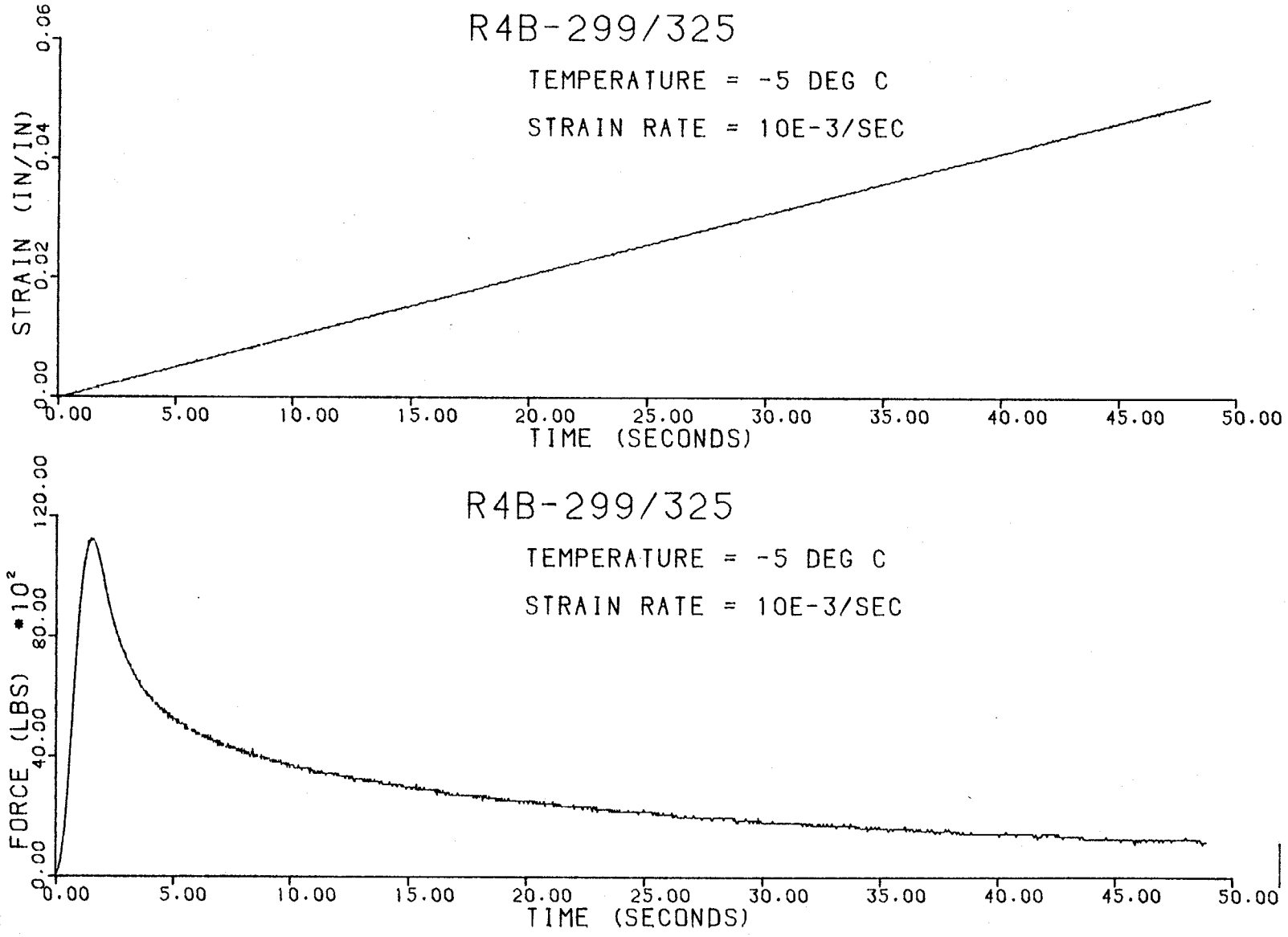


Fig. 5 - Measured strain and force histories for a $10^{-3}$/sec test.

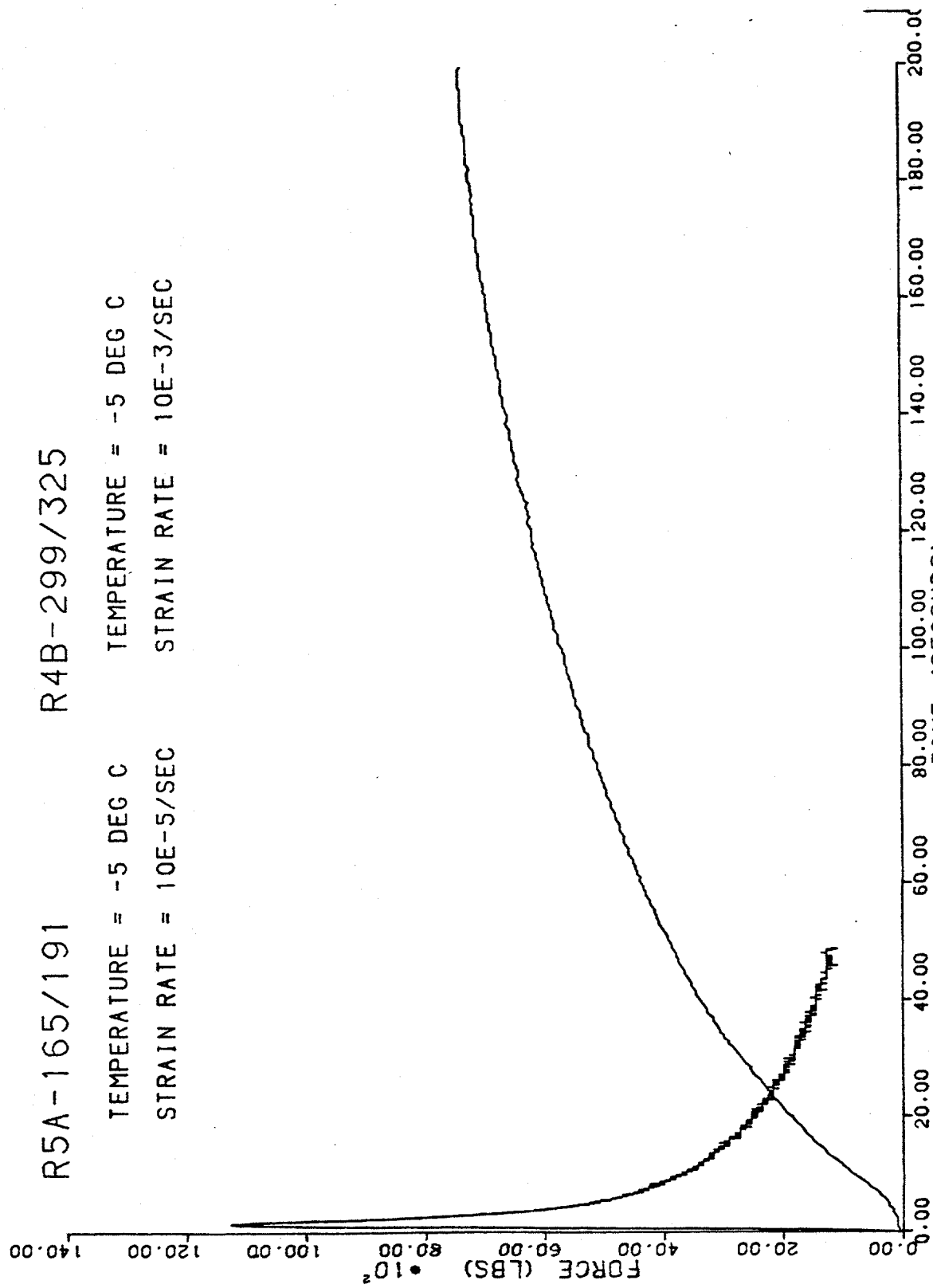


Fig. 6 - Measured force histories for a $10^{-5}$/sec and $10^{-3}$/sec test on the same coordinate axes.

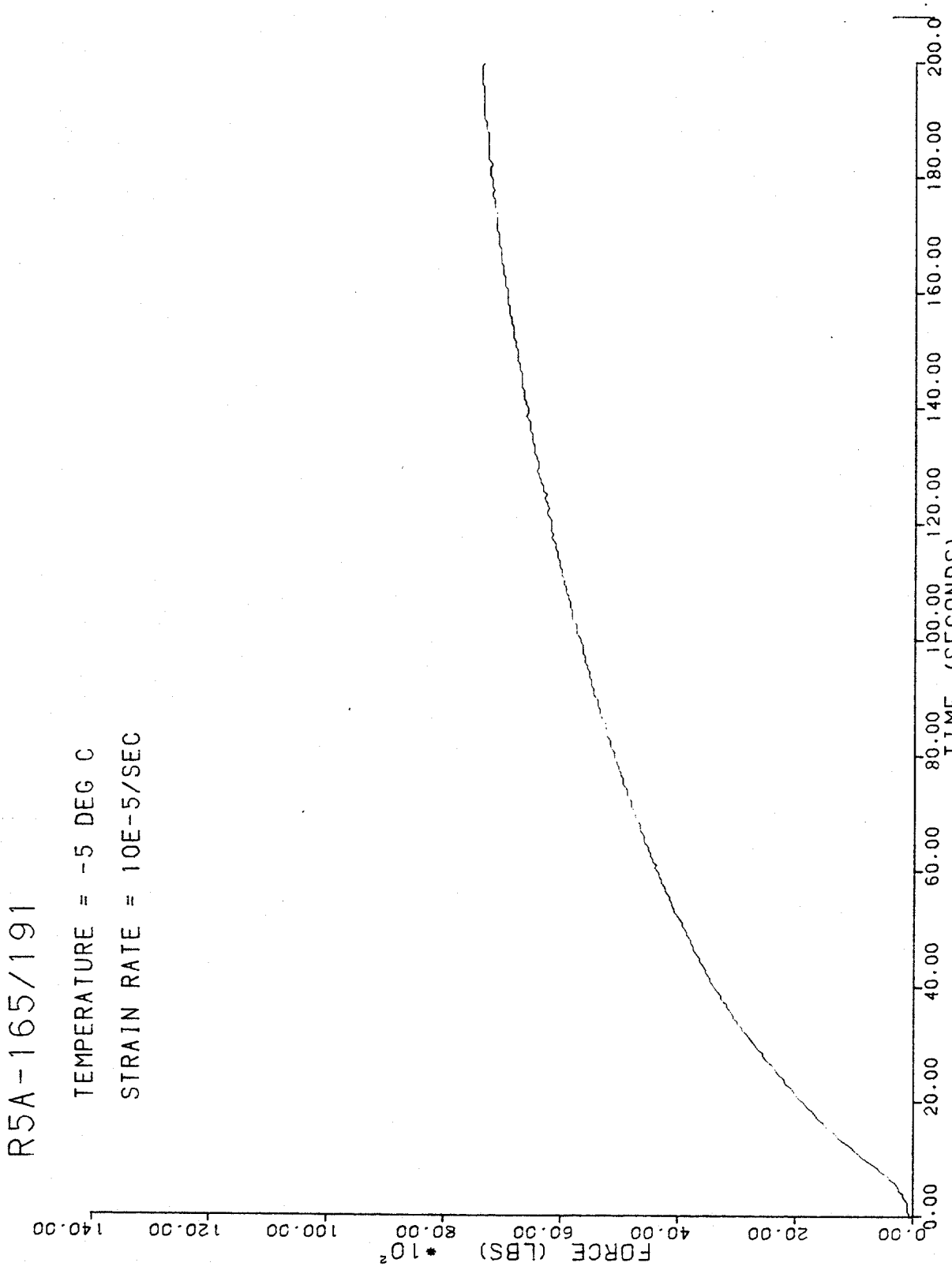


Fig. 7 - Enlarged view near the origin of the force history for a $10^{-5}$/sec test.

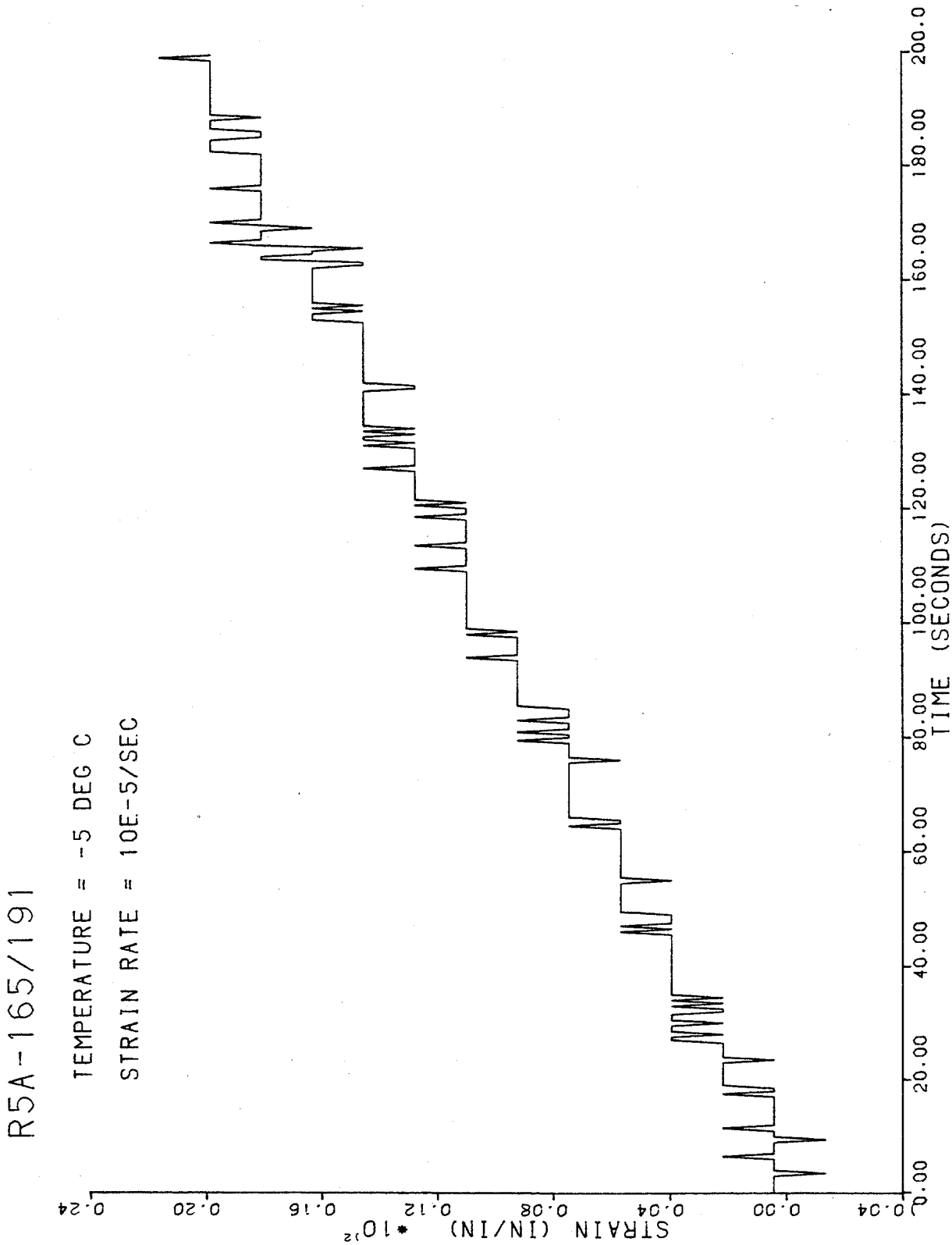


Fig. 8 - Enlarged view near the origin of the strain history for a $10^{-5}$/sec test.

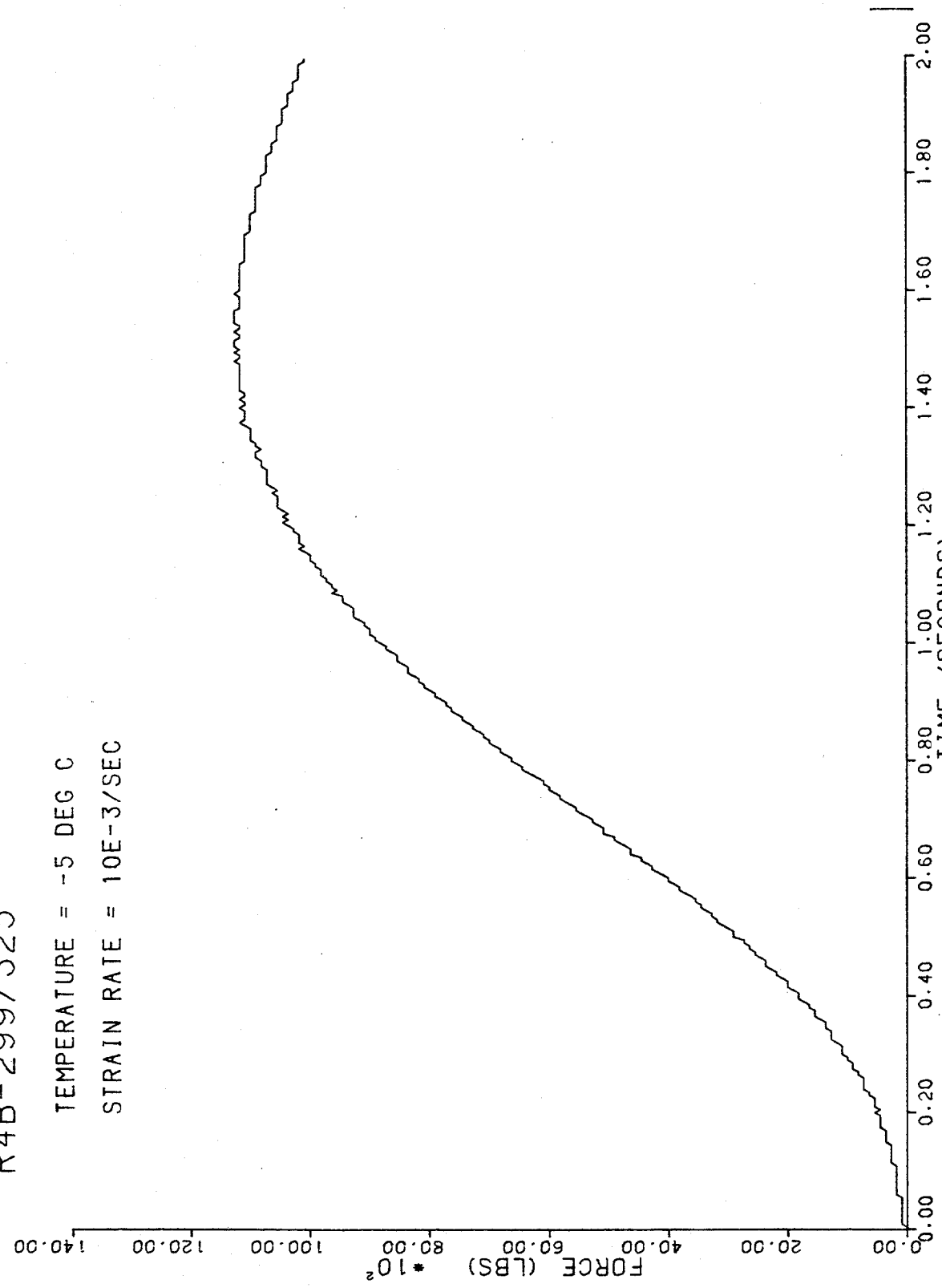


Fig. 9 - Enlarged view near the origin of the force history for a $10^{-3}$/sec test.

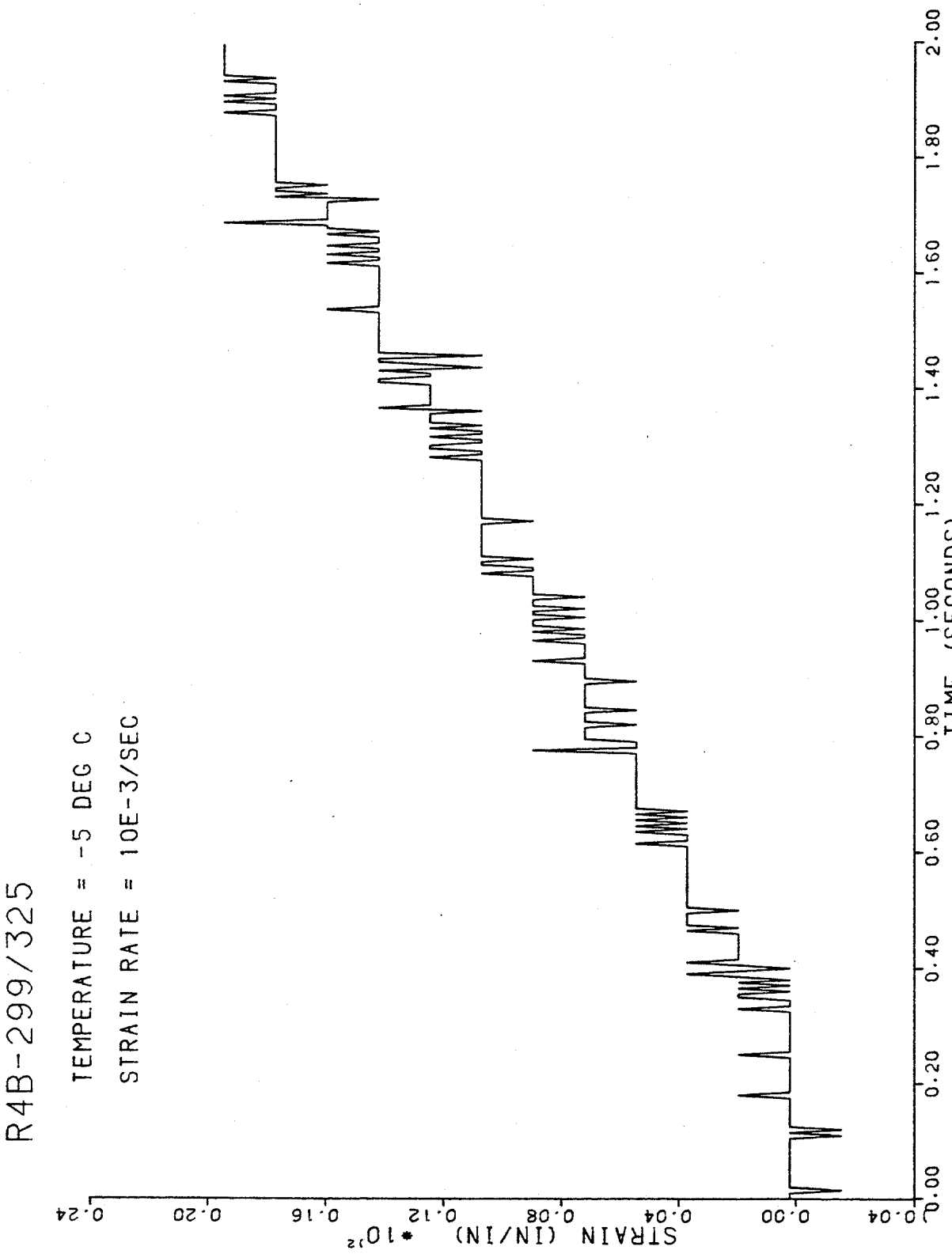


Fig. 10 - Enlarged view near the origin of the strain history for a $10^{-3}$/sec test.

With the previous problems in mind, procedures were developed to accomplish the following tasks:

1. Obtain accurate measurement of the mechanical properties. The properties of major interest from the stress-strain curves are the peak stress, the maximum slope, and the residual stress.
2. Develop a systematic method to resolve the discrepancy in the start time of the force and axial displacement measurements.
3. Generate stress-strain curves whose initial slope is the maximum slope. In doing this, we are in effect editing out the initial positive curvature in the data. Although it is recognized that this feature is an intrinsic material property in geological materials such as rock, we do not feel that the exclusion of this feature will have an effect on ice loads calculated from these edited stress-strain curves.

The subroutine ICSVKU finds cubic splines which minimize the least squares error of the entire curve. This, however, does not guarantee a good local fit. When applying the subroutine to the entire data set of digitized points, good fits are consistently obtained for the points beyond the peak force and poor fits are found for the points up to and around the peak force. The poor fit at the beginning is a result of the subroutine's preference to fit the smooth portion of the curve beyond the peak force rather than the initial portion where the slope changes rapidly from zero at t=0, reaches a maximum, and goes back to zero at the peak. It is by far easier to minimize the global least squares error by finding a good fit in the smooth post peak area where a majority of the points are located rather than fit well the few points near the origin. Attempts at improving the initial fit by adding more knots near the origin or weighing the initial part with more points failed to achieve consistent results.

To insure an accurate curve fit for the beginning of the force-time data set and hence an accurate measurement of the maximum slope, a primary smoothing is made for the initial part of the data only. This is done by creating a subset of points from the entire data set for each

strain rate. For the $10^{-5}$/sec strain rate all points for the first 40 sec comprise the subset for primary smoothing. The subset for the $10^{-3}$/sec tests consists of all points to the peak minus the first and last few points to eliminate the portions of the subset which would have zero slopes. The resulting subsets for each strain rate then form a smooth monotonically increasing data function which can be accurately fitted with splines. The subset for each strain rate is then divided into four intervals by selecting five equally spaced knots. Cubic splines are then found for each interval and the maximum slope is found by calculating the slope at the inflection point. Figures 11 and 12 show the data points in each subset, the fitted curve, and the tangent at the point of inflection for the primary smoothing.

A secondary smoothing is then made by creating another data subset for each strain rate consisting of all points to the right of the inflection point. The first few points of the subset are then deleted to insure that the initial slope of the secondary smoothing is less than the previously calculated maximum slope. The $10^{-5}$/sec data subset is divided into ten intervals and the $10^{-3}$/sec data set is divided into nine intervals. Cubic splines are then found for each interval. These splines are then considered final for that portion of the force-time curve.

The next task is to construct an additional spline which connects the initial point of the secondary smoothing with the time axis. This spline is constructed without regard to the data points prior to the initial point of the secondary smoothing since those points represent the portion of the curve with positive curvature.

The first step in this procedure is to shift the knot index, i, of the quantities returned by the subroutine for the secondary smoothing. The shift is made by increasing the index by one, so that $t_i$, becomes $t_2$, $y_1$, becomes $y_2$, $C_{1j}$, j=1,3, becomes $C_{2j}$, etc. The secondary smoothing is now described by (k-1) splines $S_i(\xi_i)$, i=2, k. A schematic diagram illustrating the additional spline along with the secondary smoothing is shown in Figure 13.

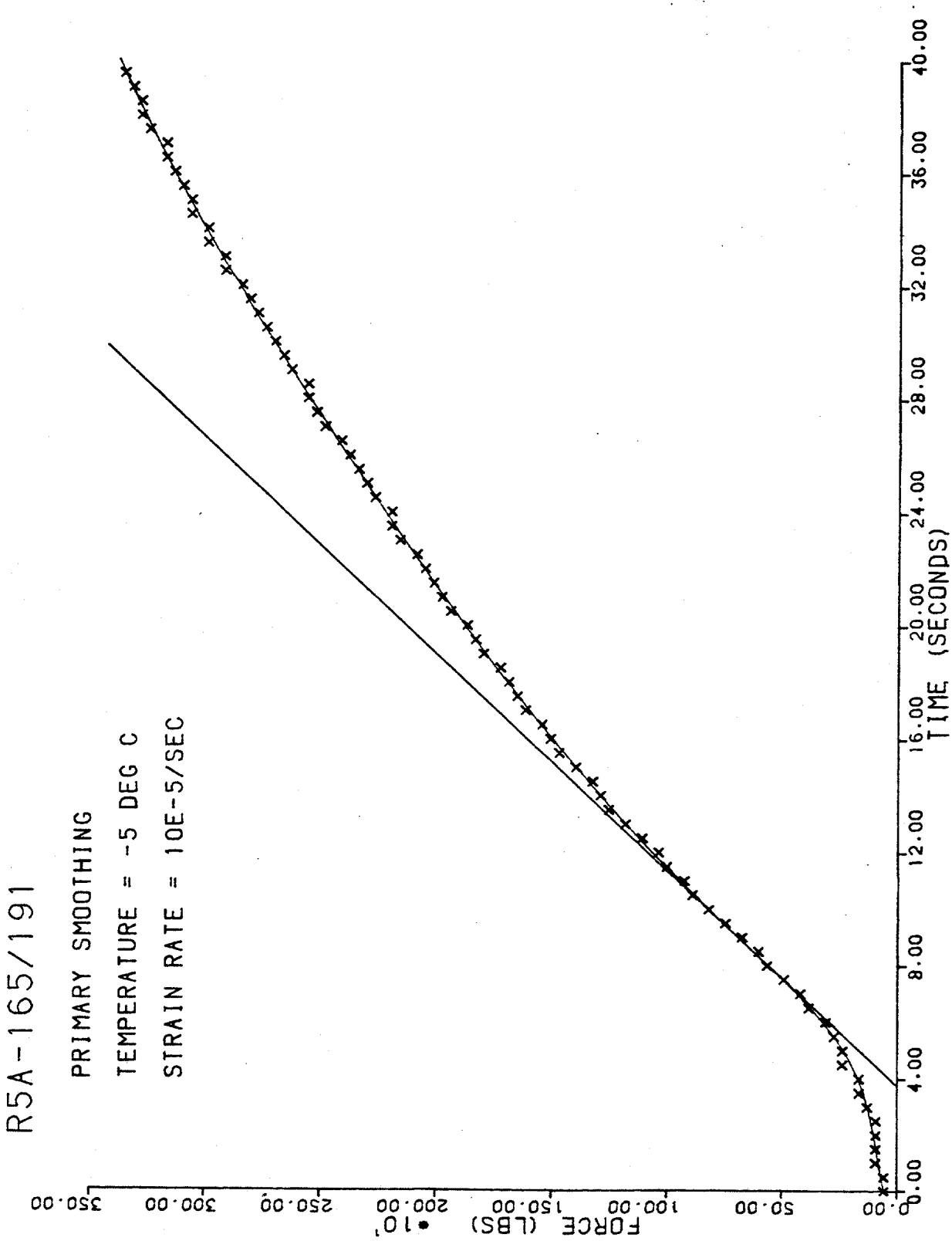


Fig. 11 - Primary smoothing and tangent at the inflection point for a $10^{-5}$/sec test.

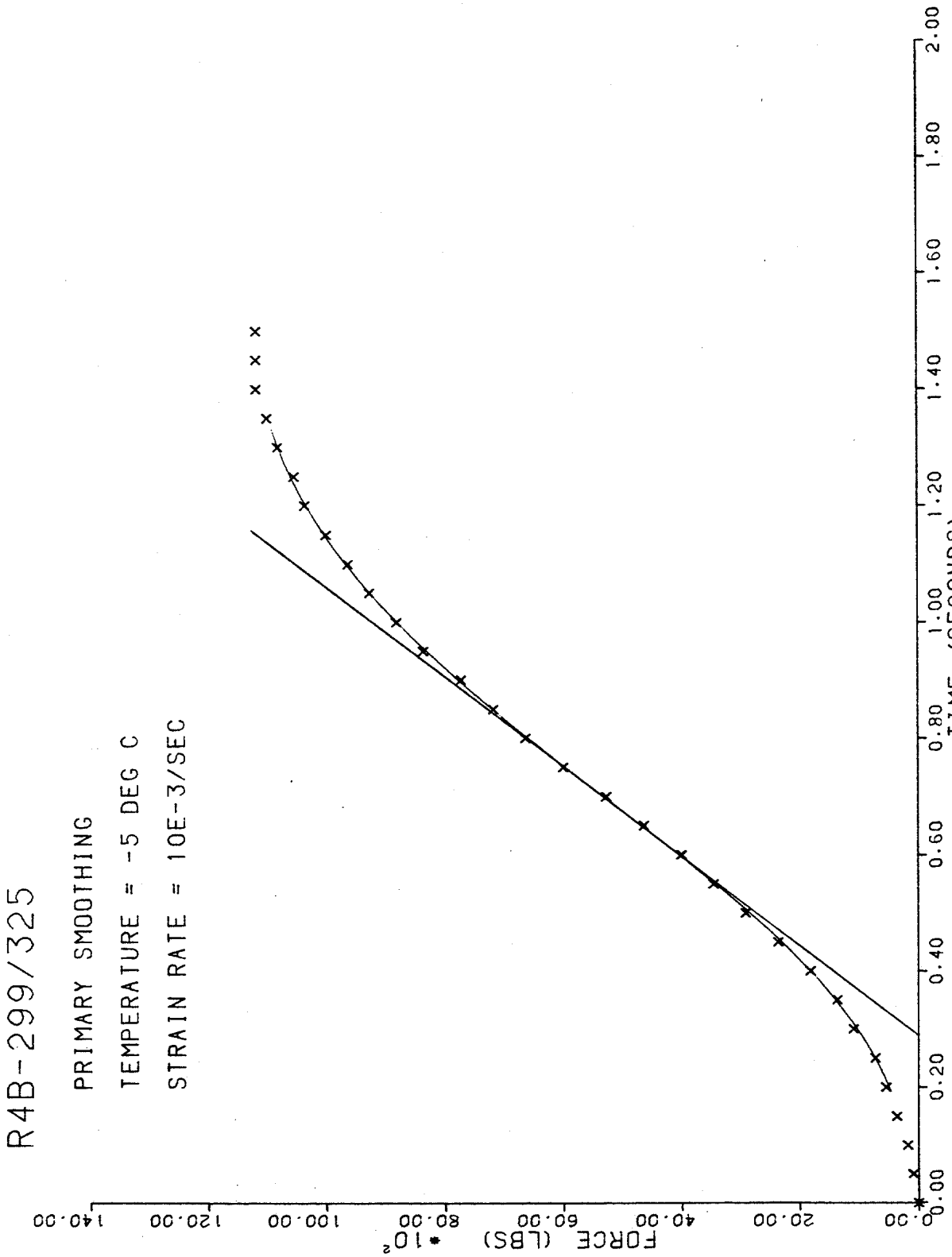


Fig. 12 - Primary smoothing and tangent at the inflection point for a $10^{-3}$/sec test.

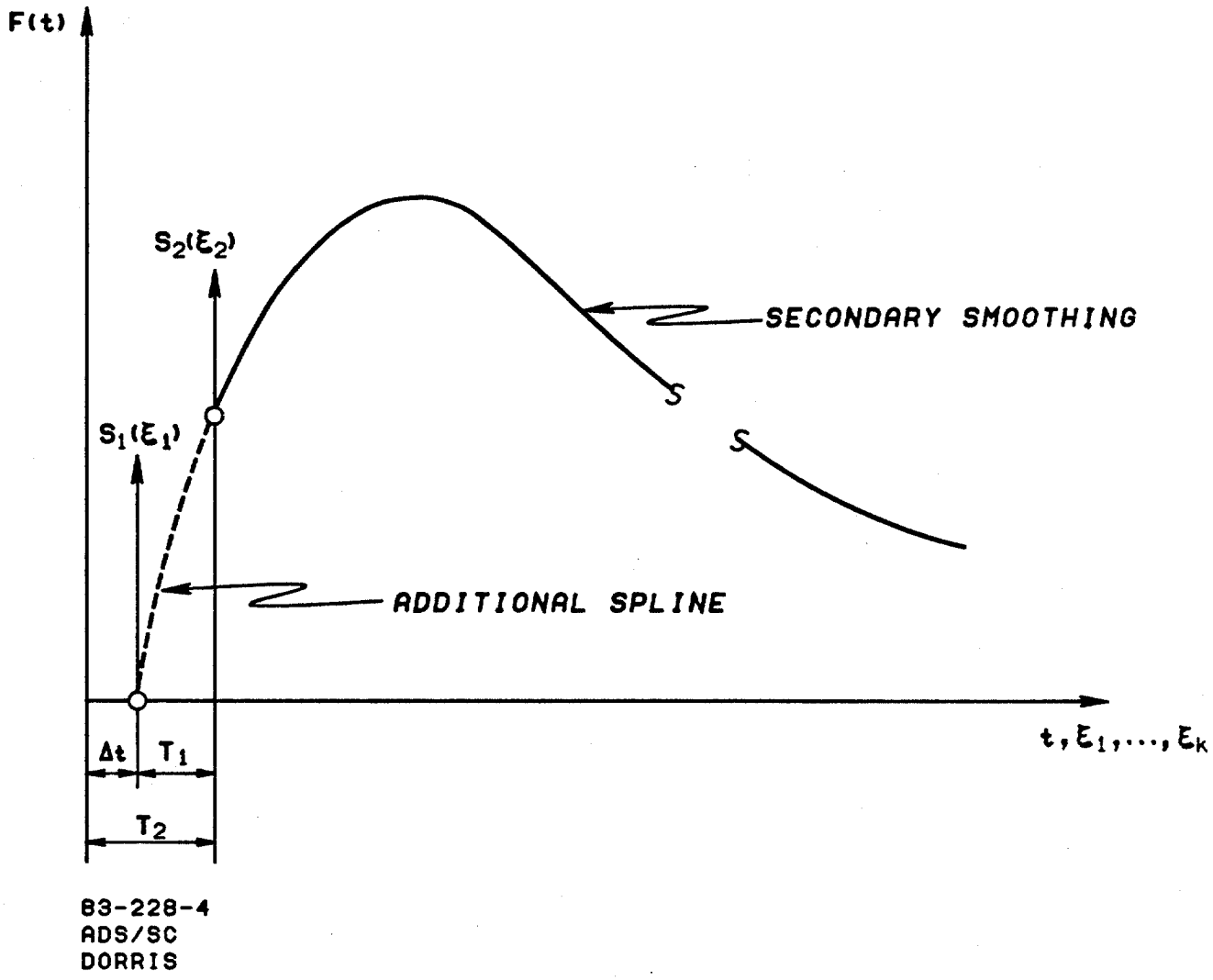


Fig. 13 - Schematic diagram of the location of the additional spline with respect to the secondary smoothing.

To construct the additional spline, $S_1(\xi_1)$, a local coordinate system is set up at the point $(t_2-T_1,0)$. The independent variable for this coordinate system is $\xi_1$ and covers the range $0\leq\xi_1\leq T_1$. The spline, $S_1(\xi_1)$, is found by constructing a cubic polynomial which satisfies the following conditons:

$$
\begin{aligned}
&1. \quad S_1(0) = 0 \\
&2. \quad S_1'(0) = F'_{max} \\
&3. \quad S_1''(0) = F''_o \\
&4. \quad S_1(T_1) = S_2(0) = y_2 \\
&5. \quad S_1'(T_1) = S_2'(0) = C_{21} \\
&6. \quad S_1''(T_1) = S_2''(0) = 2C_{22}
\end{aligned}
\tag{2}
$$

Here $F'_{max}$ denotes the maximum slope calculated from the primary smoothing. Although the cubic polynomial which we are trying to construct is described by four unknown constants, the six conditions shown above can be satisfied since the quantities $T_1$ and $F''_o$ are also considered as unknowns.

Successive elimination of the unknowns in the above conditions can yield a quadratic equation in $F''_o$ with the coefficients being algebraic combinations of the known quantities $F'_{max}$, $y_2$, $C_{21}$, and $C_{22}$. Solution of this quadratic equation will yield two solutions for $F_o$. If one of these solutions is negative then that solution is chosen to be the correct solution. With $F''_o<0$, we are guaranteed that the curvature of $S_1(\xi_1)$ will be negative since we have required that the initial slope of the secondary smoothing be less than $F'_{max}$. Once the additional spline, $S_1(\xi_1)$, is determined the smoothing procedure is complete. Figure 14 illustrates the smooth curve obtained for the $10^{-5}$/sec test using this procedure. Figure 15 is an enlarged view of this curve to illustrate the initial negative curvature of the smooth curve and the continuity at the initial point of the secondary smoothing.

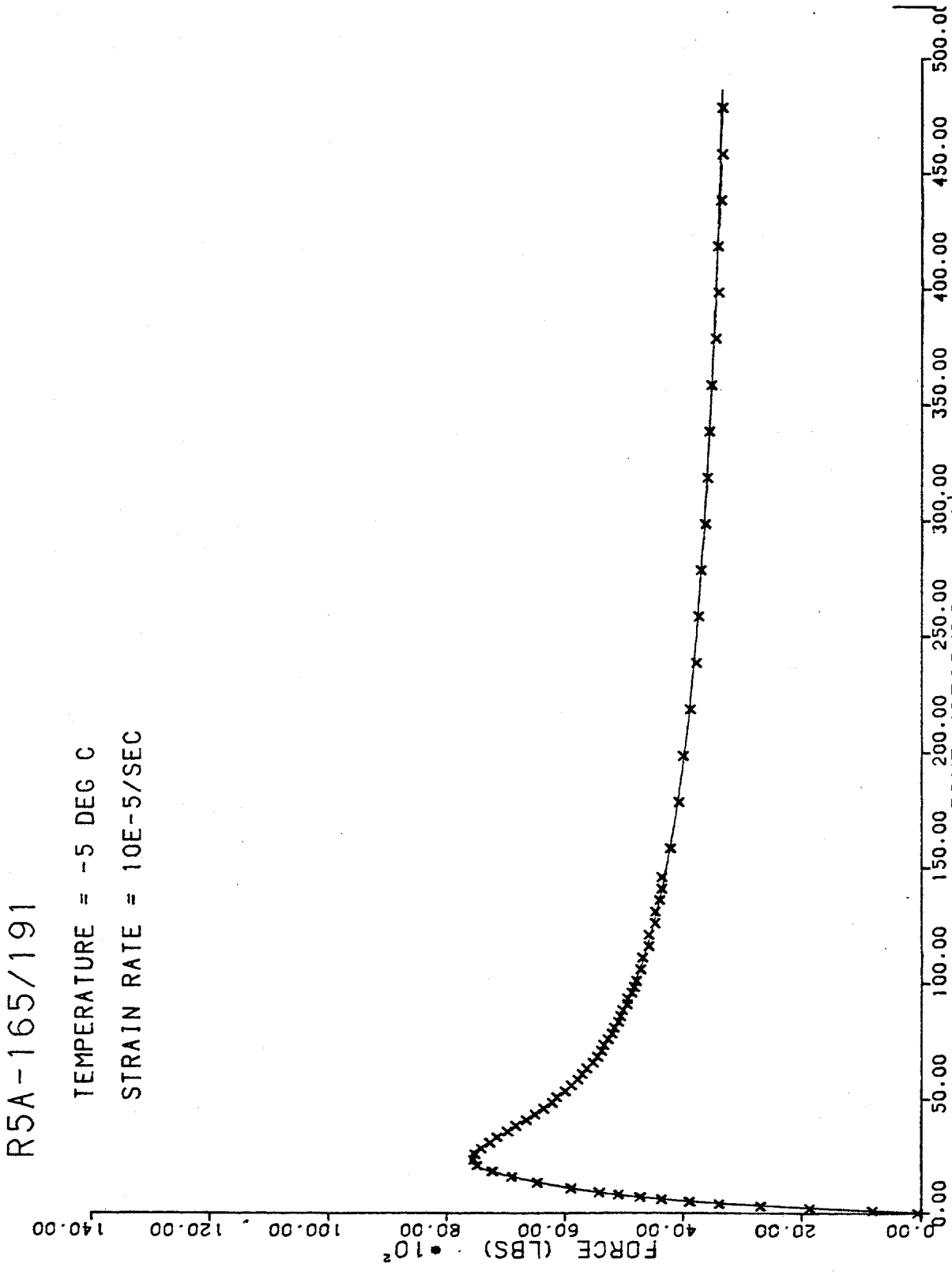


Fig. 14 - Smooth curve obtained for a $10^{-5}$/sec test using one additional knot to supplement the secondary smoothing.

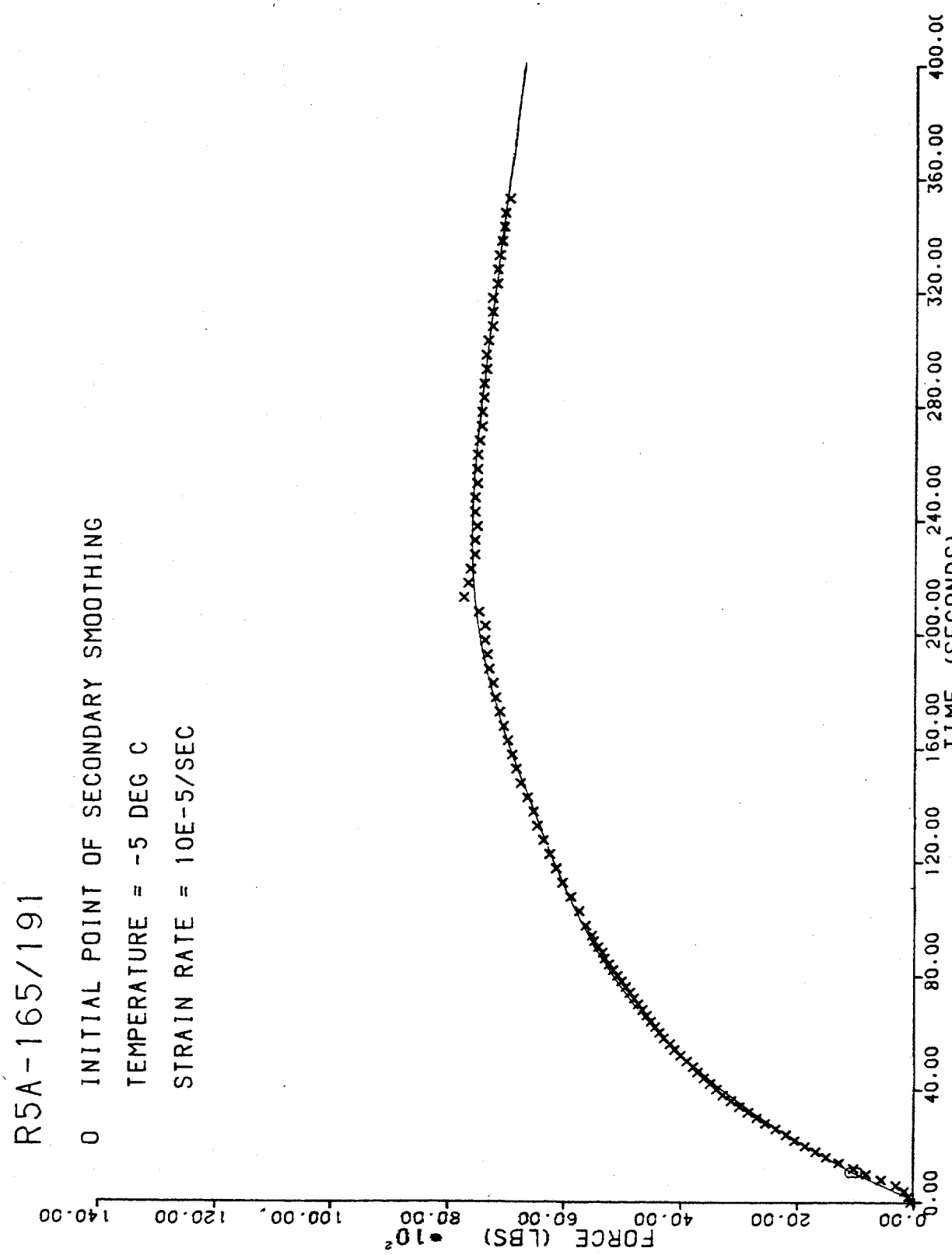


Fig. 15 - Enlarged view of Figure 14 near the origin.

In the event that the quadratic equation for $F_o''$ yields two positive solutions or two imaginary solutions, the conditions in Equations (2) can be relaxed by adding two splines to the secondary smoothing instead of one. In this case the knot indices, i, for $t_i$, $y_i$, and $C_{ij}$, j=1,3, are shifted by two. Figure 16 illustrates the location of the additional splines after the index shift has been made.

To construct the spline adjacent to the initial point of the secondary smoothing, a local coordinate system is set up at the point $(t_3-T_2,0)$. The independent variable for this coordinate system is $\xi_2$ and covers the range $0 \leq \xi_2 \leq T_2$. The spline, $S_2(\xi_2)$ is found by constructing a cubic polynomial which satisfies the following conditions:

$$
\begin{aligned}
&1. \quad S_2'(0) = F'_{max}, \\
&2. \quad S_2''(0) = 0, \\
&3. \quad S_2(T_2) = S_3(0) = y_3, \\
&4. \quad S_2'(T_2) = S_3'(0) = C_{31}, \\
&5. \quad S_2''(T_2) = S_3''(0) = 2C_{32}.
\end{aligned}
\tag{3}
$$

The above five conditions are sufficient to solve for the four unknown constants of the cubic polynomial and the unknown time quantity, $T_2$. Since the inital point of the secondary smoothing is a few points to the right of the inflection point of the primary smoothing, the quantity, $(t_3-T_2)$ roughly corresponds to the time at which the inflection point occurs in the experimental data.

In a similar manner the spline to the left of $S_2(\xi_2)$ is found by setting up a local coordinate system at the point, $(t_3-T_2-T_1,0)$ for the independent variable, $\xi_1$, which covers the range, $0 \leq \xi_1 \leq T_1$. The spline $S_1(\xi_1)$ is found by constructing a cubic polynomial which satisfies the following conditions:

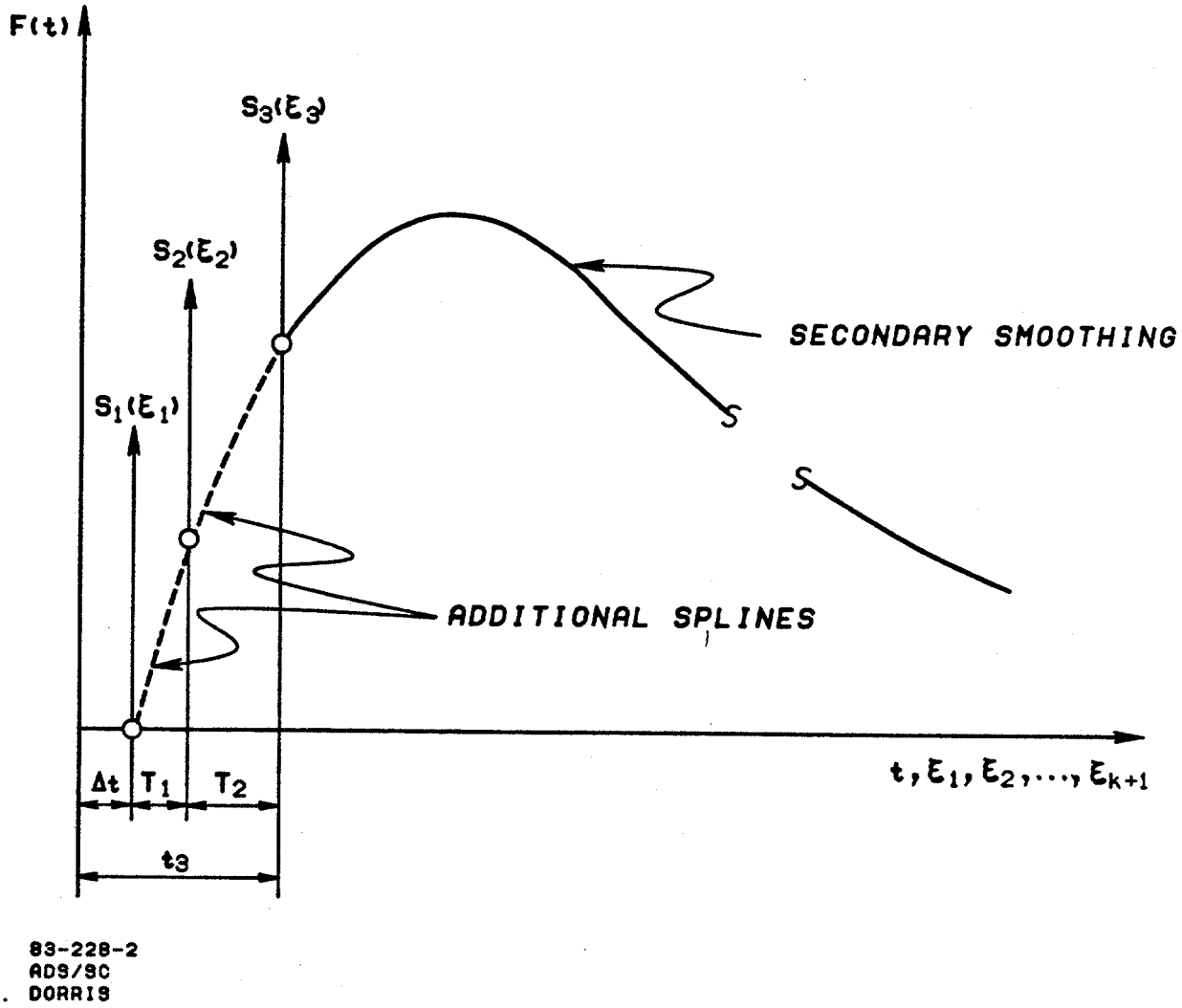


Fig. 16 - Schematic diagram of the location of the two additional knots with respect to the secondary smoothing.

$$
\begin{aligned}
&1. \quad S_1(0) = 0, \\
&2. \quad S_1'(0) = F_{max}', \\
&3. \quad S_1''(0) = 0, \qquad (4) \\
&4. \quad S_1(T_1) = S_2(0), \\
&5. \quad S_1'(T_1) = S_2'(0) = F_{max}'.
\end{aligned}
$$

These five conditions are sufficient to find the four unknown constants of the cubic spline, $S_1(\xi_1)$, and the unknown time quantity, $T_1$. Note that the application of conditions 3 and 5 in Equations (3) collapses the cubic polynomial into a linear curve which automatically forces continuity of the second derivative at $T_1$.

After the two additional splines are found the smoothing procedure is completed. Figure 17 illustrates the type of fit obtained for the $10^{-3}$/sec test using the additional two knot procedure. Again, an enlarged view of the fit is shown in Figure 18 to illustrate the initial linear portion of the smooth curve and the continuity at the initial point of the secondary smoothing.

The particular technique used to determine the initial portion of the smooth curve depends on the initial conditions of the secondary smoothing and the maximum slope found in the primary smoothing. As a general rule, the shape of the $10^{-3}$/sec tests is such that two additional knots are required to supplement the secondary smoothing. On the other hand, the $10^{-5}$/sec tests seem to favor the technique requiring only one additional knot although a few of those tests were found which required two knots to complete the smoothing.

Regardless of the technique used to find the initial portion, the start time of each test is determined by shifting the global force-time coordinate axes to coincide with the local axes, $(\xi_1, S(\xi_1))$. The shift is easily made with the coordinate transformation, $\bar{t}=t-\Delta t$, where $\Delta t=t_2-T_1$ when one additional knot is required and $\Delta t=t_3-T_2-T_1$ when two additional knots are required. The quantity $\Delta t$ is illustrated for each technique in Figures 13 and 16. The previously determined splines are

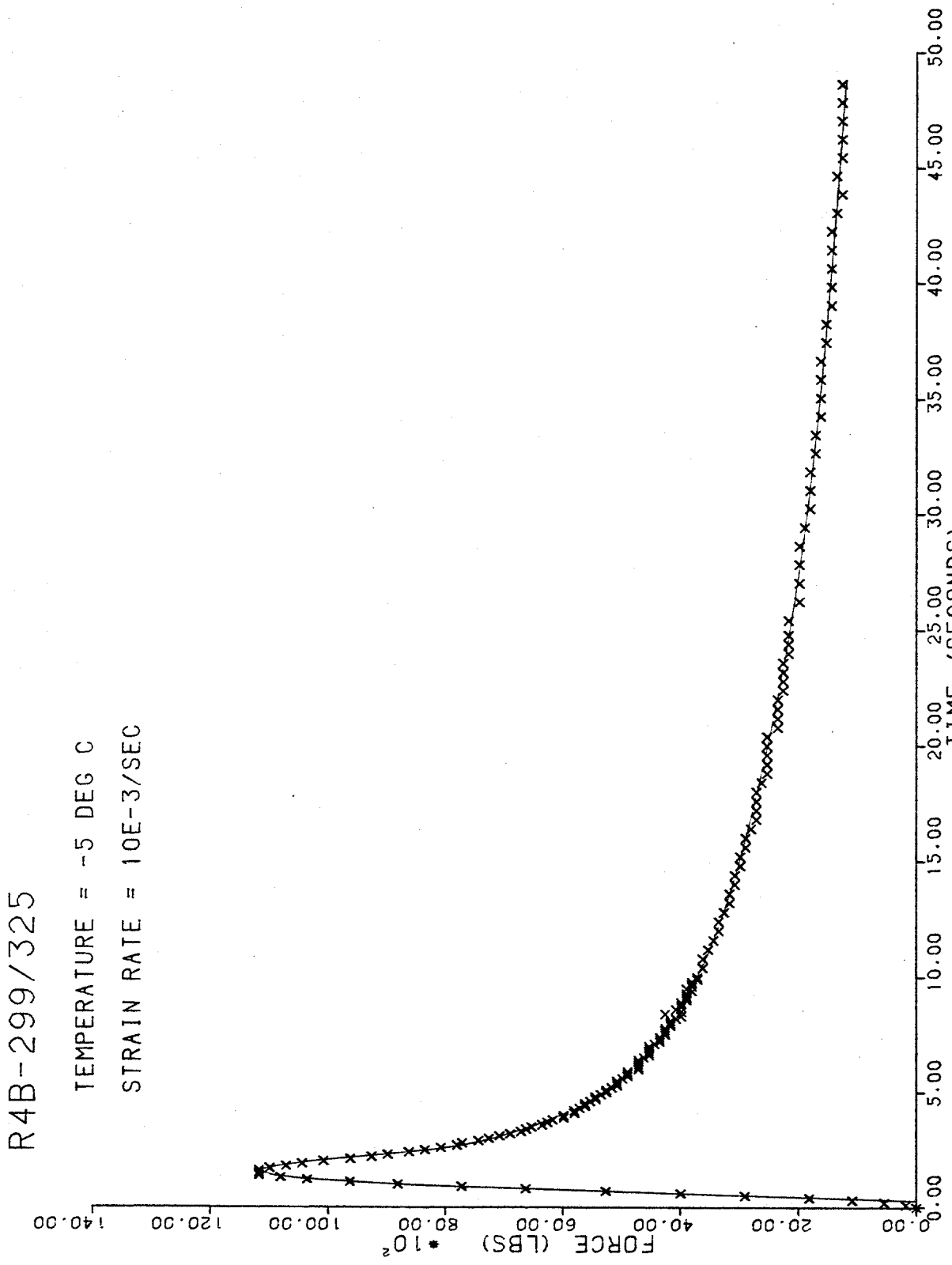


Fig. 17 - Smooth curve obtained for a $10^{-3}$/sec test using two additional knots to supplement the secondary smoothing.

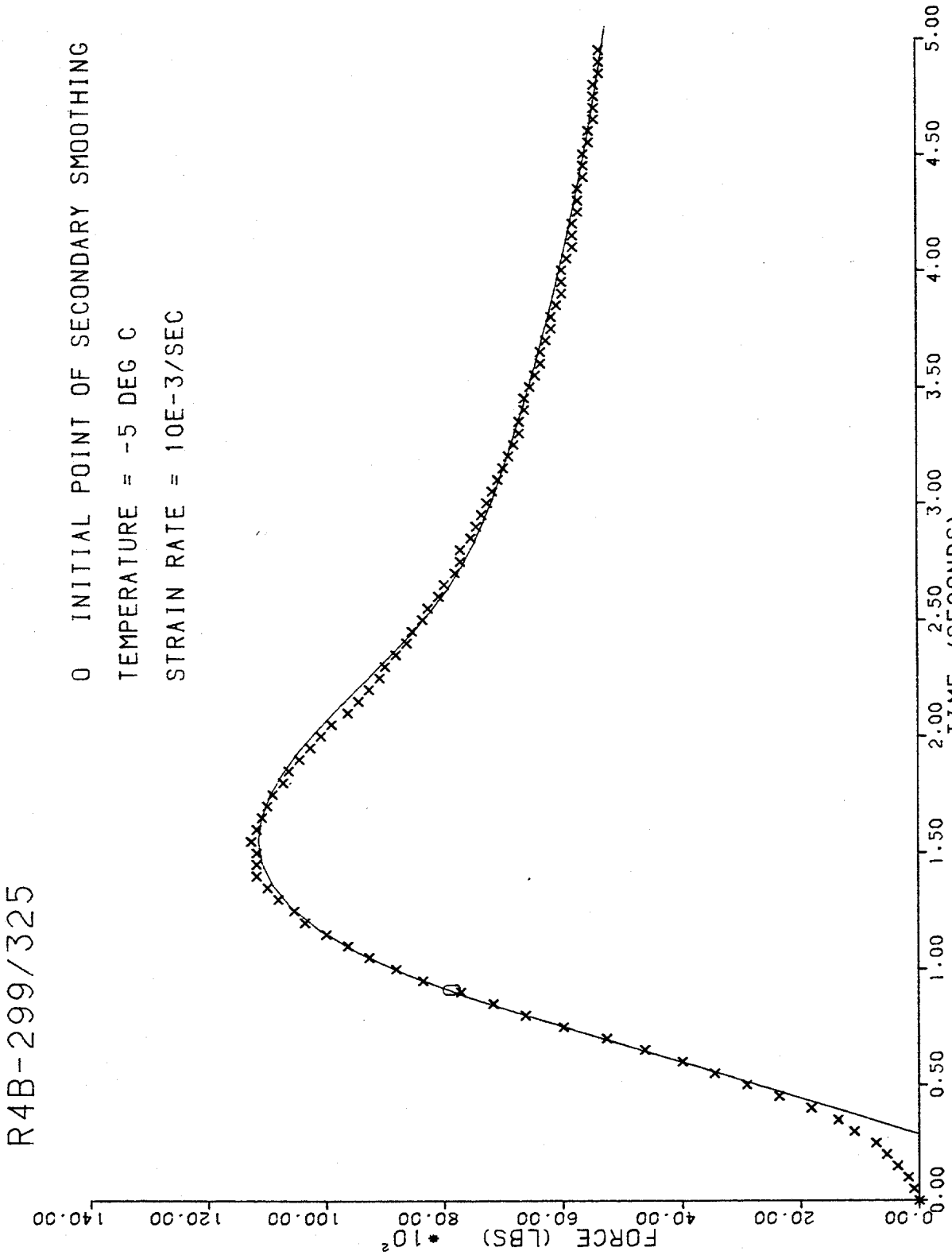


Fig. 18 - Enlarged view of Figure 17 near the origin.

valid in the new coordinate system as long as a similar transformation is made for each knot, i.e. $\bar{t}_i = t_i - \Delta t$. The amount of the time shift, $\Delta t$, is on the order of 8 sec for the $10^{-5}$/sec tests and 0.2 sec for the $10^{-3}$/sec tests. In each case the time shift is within the uncertainity of the start time.

After the time shift, the resulting function $F(\bar{t})$ represents the force history of the entire test. If the final number of knots is m, then $F(\bar{t})$ will consist of (m-1) branches, $S_i(\xi_i)$, defined on the intervals, $0 \leq \xi_i \leq \bar{t}_{i+1} - \bar{t}_i$, where $\xi_i = \bar{t} - \bar{t}_i$. The function, $F(\bar{t})$, is continuous and has continuous first and second derivatives at every point. Furthermore, the maximum slope of $F(\bar{t})$ occurs at the origin and is equal to the maximum slope of the experimental data. The composite function is completely defined by the knots, $\bar{t}_i$, i=1,m, the initial value of each spline, $y_i$, i=1,(m-1), and the spline coefficients, $C_{ij}$, i=1,(m-1), j=1,3. These values are tabulated in data files for each test and are shown in Table 1 for test number R5A-165/191 and Table 2 for test number R4B-299/325.

As a final step, the strain history is shifted by the amount, $\Delta t$. Two knots are chosen at the beginning and end of the strain history and a cubic spline is found by calling the subroutine. This step is unnecessary since the strain history is linear for a constant strain rate test, but it does provide a check on the test strain rate. The check is made by comparing the coefficients returned by the subroutine. If the cubic and quadratic coefficients are several orders of magnitude smaller than the linear coefficient and if the linear coefficient is within 1% of the test strain rate, then the test is considered valid.

Once this check is completed, the force-time curve, $F(\bar{t})$ is used to generate the stress-strain curve by scaling the coordinate axes. The force axis is divided by the original cross sectional area of the test sample and the time axis is multiplied by the test strain rate. The stress-strain curve for test number R5A-165/191 is shown in Figure 19 and the stress-strain curve for test number R4B-299/325 is shown in Figure 20.

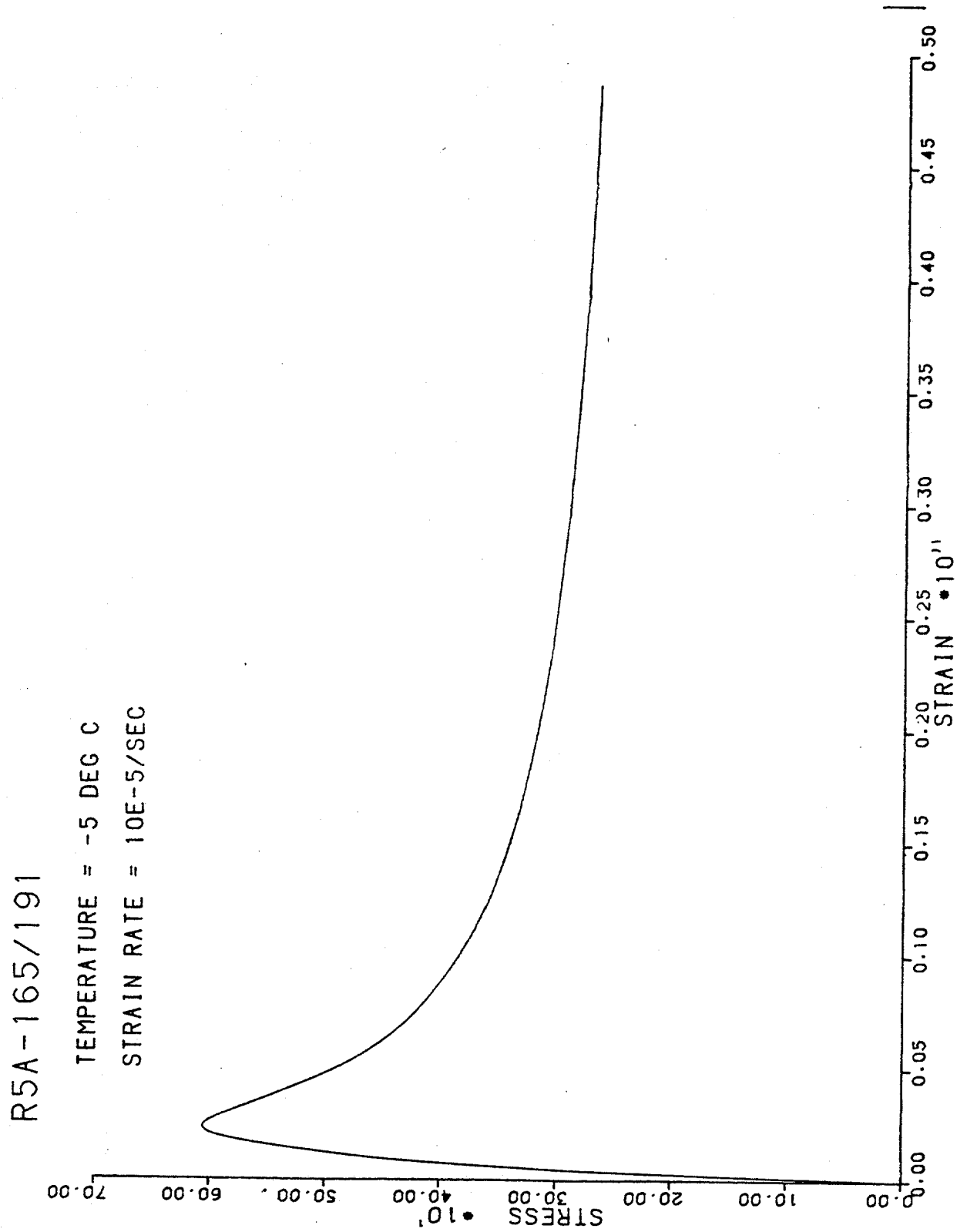


Fig. 19 - Final stress-strain curve for a $10^{-5}$/sec test.

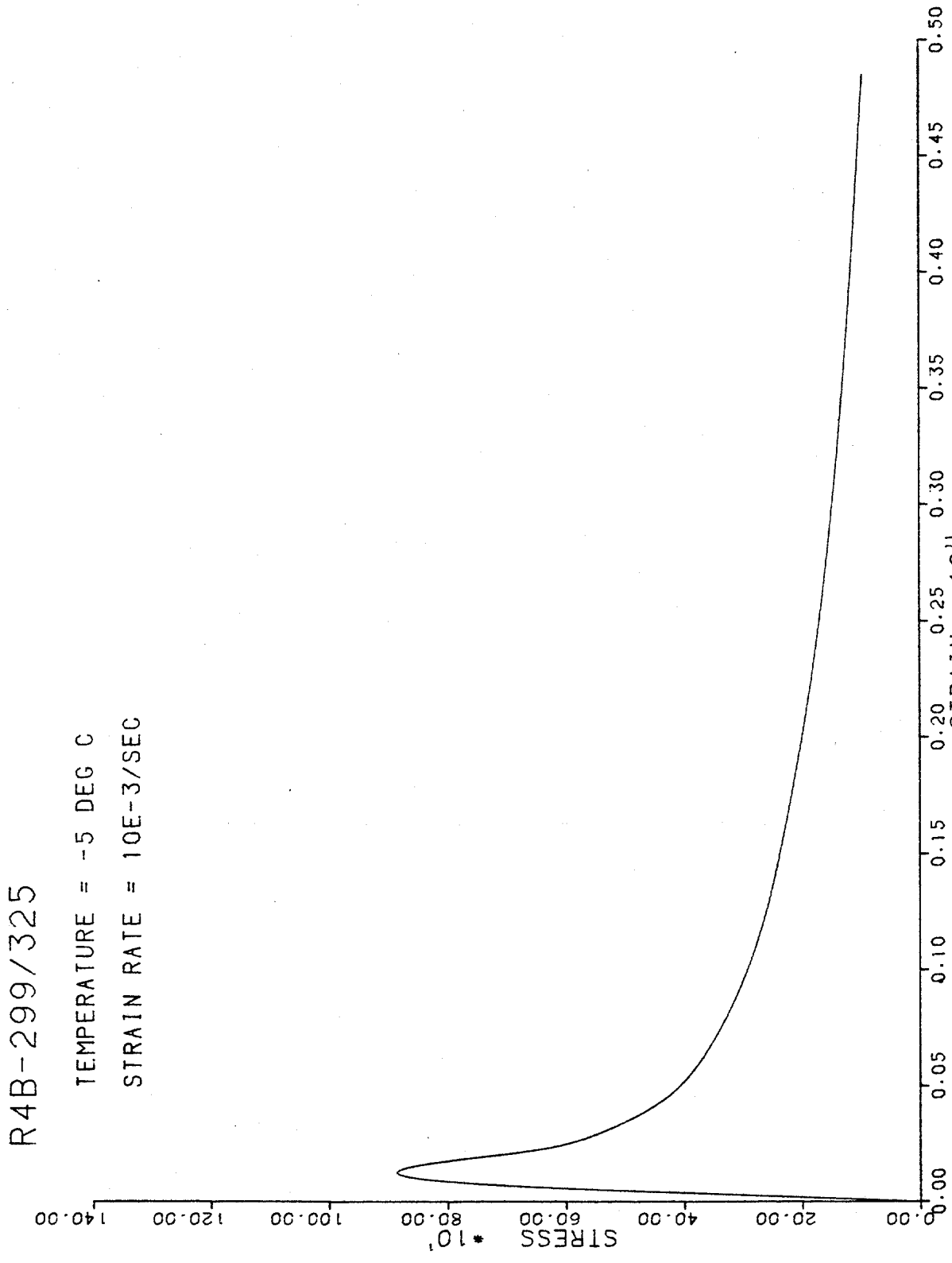


Fig. 20 - Final stress-strain curve for a $10^{-3}$/sec test.

Table 1

SPLINE PARAMETERS FOR R5A-165/191

R5A-165/191
TEMPERATURE = -5 DEG C
STRAIN RATE = 10E-5/SEC

| I | T(I) | Y(I) | C(I,1) | C(I,2) | C(I,3) |
|---|---|---|---|---|---|
| 1 | .00000 | .00000 | 131.31 | -3.7794 | .12883 |
| 2 | 8.1923 | 892.91 | 95.323 | -.61325 | .16520-02 |
| 3 | 69.872 | 4827.0 | 38.528 | -.30757 | .16499-02 |
| 4 | 131.55 | 6420.5 | 19.417 | -.22724-02 | -.81213-03 |
| 5 | 193.23 | 7418.9 | 9.8675 | -.15255 | .48903-03 |
| 6 | 223.23 | 7590.8 | 2.0350 | -.10854 | .49065-03 |
| 7 | 293.32 | 7369.2 | -5.9486 | -.53647-02 | .26355-04 |
| 8 | 463.63 | 6330.7 | -5.4827 | .81005-02 | -.59914-05 |
| 9 | 837.77 | 5099.6 | -1.9372 | .13757-02 | -.48428-06 |
| 10 | 1571.7 | 4227.4 | -.70050 | .30945-03 | -.72329-07 |
| 11 | 2711.9 | 3723.7 | -.27691 | .62030-04 | -.64907-08 |
| 12 | 4869.8 | | | | |

Table 2

SPLINE PARAMETERS FOR R4B-299/325

R4B-299/325
TEMPERATURE = -5 DEG C
STRAIN RATE = 10E-3/SEC

| I | T(I) | Y(I) | C(I,1) | C(I,2) | C(I,3) |
|---|---|---|---|---|---|
| 1 | .00000 | .00000 | 12941. | .00000 | .00000 |
| 2 | .47849 | 6191.9 | 12941. | .00000 | -31167. |
| 3 | .60234 | 7735.3 | 11506. | -11580. | 2921.5 |
| 4 | .84734 | 9902.3 | 6358.2 | -9432.8 | 2842.6 |
| 5 | 1.0923 | 10936. | 2248.0 | -7343.5 | 2973.9 |
| 6 | 1.3423 | 11085. | -866.16 | -5113.1 | 2759.8 |
| 7 | 1.5923 | 10592. | -2905.2 | -3043.2 | 2890.7 |
| 8 | 2.2558 | 8169.3 | -3126.2 | 2710.2 | -1346.4 |
| 9 | 2.8625 | 6969.6 | -1324.4 | 259.67 | -22.095 |
| 10 | 6.4561 | 4538.3 | -314.05 | 21.468 | -.72645 |
| 11 | 15.167 | 2951.5 | -105.41 | 2.4843 | -.27138-01 |
| 12 | 48.622 | | | | |